ISSN: 2414-1895 DOI: 10.6919/ICJE.202208_8(8).0052

Effect of Longitudinal Torsional Compound Ultrasonic Vibration on the Axial Force of Ti-6Al-4V Micro Deep Hole Drilling

Ziqiang Liu, Jinglin Tong*, Pingyan Bian, Penghui Zai, and Zhipeng Zhang

Henan Polytechnic University, Jiaozuo 454000, China

Abstract

The method of longitudinal torsional composite ultrasonic vibration drilling of tiny deep holes is proposed for the problems of large cutting force and poor quality of machined holes during the drilling of microfine deep holes of difficult-to-machine material Ti-6Al-4V. The ultrasonic-assisted drilling mechanism was analyzed, and a longitudinal torsional composite ultrasonic vibration drilling model was established by combining with the longitudinal ultrasonic vibration drilling model. And the cutting force model of main cutting edge and cross edge under longitudinal-torsional composite ultrasonic vibration was established by using micro-element method. The effect of cutting parameters and acoustic parameters on the axial force of drilling, the shape of the entrance and exit of the microhole and the quality of the hole wall were analyzed. The test results showed that the axial cutting force was significantly reduced during the longitudinal-torsional compound ultrasonic vibration drilling process; the chips were more easily broken, and the groove defects of the microhole wall were improved, smoother and the hole wall roughness was smaller. The quality of Ti-6Al-4V micro-deep hole drilled by longitudinal torsion compound ultrasonic vibration has been significantly improved.

Keywords

Longitudinal Torsional Composite; Micro Hole Drilling; Axial Force; Microelement Method.

1. Introduction

Titanium alloy has a series of excellent properties such as light weight, high strength, corrosion resistance, good thermal hardness and low temperature performance compared with traditional steel[1,2], so titanium alloy is gradually widely used in many fields such as aerospace, medical equipment, marine ships, petrochemicals, etc., and has been named "all-purpose metal" and "space metal". "Space Metal" and other titles[3-5] . However, the low thermal conductivity, poor plasticity, low modulus of elasticity and other characteristics of titanium alloy[6], resulting in its cutting performance is very poor. Especially in the tiny deep hole processing, micro drill bit into the drill will occur offset, broken[7,8] , drilling chip can not be smoothly discharged resulting in increased cutting force to damage the drill bit. These situations will lead to a series of problems such as large burrs at the entrance and exit of the processed micro-hole and poor hole wall quality.

In ultrasonic assisted drilling, ultrasonic vibration is attached to the micro drill or workpiece, which can make the drill in the drilling centering process from continuous cutting to intermittent cutting, so as to effectively avoid the fracture of the micro drill due to excessive lateral displacement[9,10] , and the drill to do ultrasonic vibration is conducive to the discharge of chips from the hole, thereby reducing the axial force, avoiding the micro hole blockage caused by drill wear and damage to the hole wall and other situations. This reduces the axial force and avoids micro-hole clogging, which can cause wear and damage to the hole wall.

ISSN: 2414-1895 DOI: 10.6919/ICJE.202208_8(8).0052

FENG P F[11] et al. experimentally investigated hole exit tearing defects due to drilling during rotary ultrasonic machining of C/SiC composites and concluded that rotary ultrasonic drilling reduced hole exit tearing defects and cutting forces; increasing spindle speed and ultrasonic amplitude or decreasing feed rate helped to further reduce hole exit tearing coefficient. Zhong[12] et al. conducted tests on OCr17Ni4Cu4Nb stainless steel material on a designed ultrasonic axial vibration drilling test rig. The experimental results showed that compared with normal drilling, ultrasonic vibration drilling reduced axial force and torque, obtained good chip breaking and chip removal, improved the stability of the drilling process and prolonged the tool life. ZHANG[13] et al. investigated the cutting thickness and chip morphology of ultrasonic vibration micro-hole drilling. Ekrem Oezkaya[14] et al. analyzed the simulation of chip formation and mechanical loading during deep hole drilling with micro single lip under different cooling lubricant pressure.

In order to explore the characteristics of the trajectory of the main cutting edge and the basic principle of the axial force in longitudinal twist compound ultrasonic vibration micro-deep hole drilling, the trajectory of the cutting edge in longitudinal twist compound ultrasonic vibration drilling is analyzed and the principle of the reduction of the axial force in longitudinal twist compound ultrasonic vibration drilling is explained by combining the periodic characteristics of ultrasonic waves and the vibration model. In addition, the effects of cutting parameters and acoustic parameters on axial force, microhole entrance and exit burrs and hole wall quality in longitudinal torsional composite ultrasonic vibration microhole drilling were also investigated.

2. Analysis of the Mechanism of Longitudinal Torsion Compound Ultrasonic Vibration Micro-hole Drilling

2.1 Trajectory Equation of the Main Cutting Edge

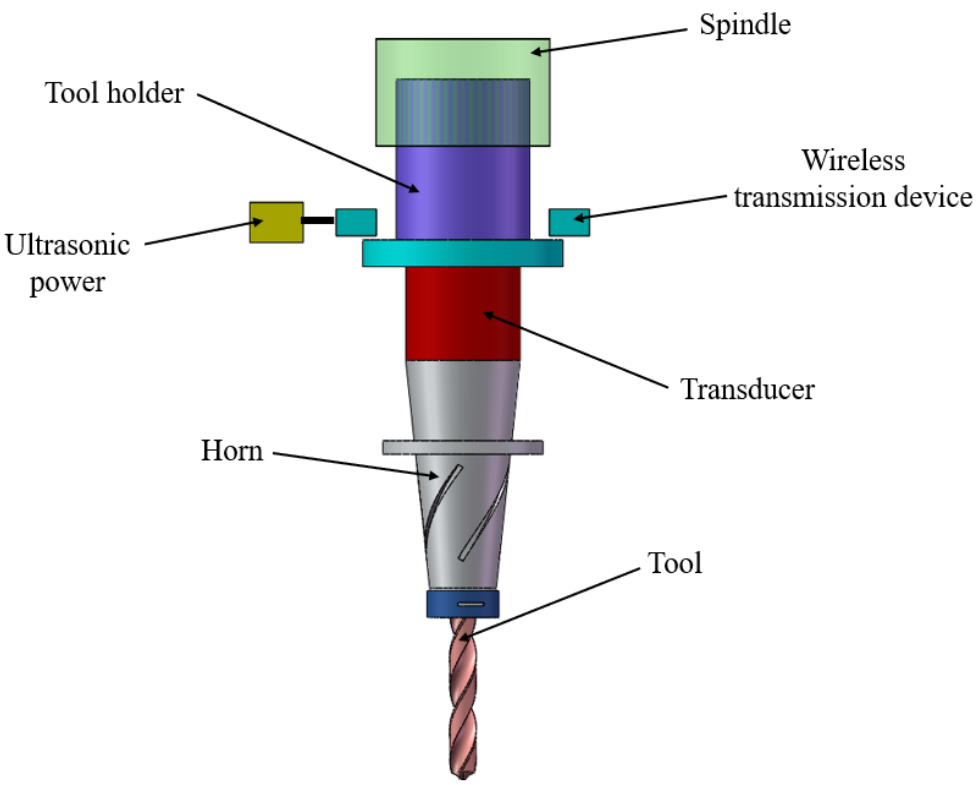

Figure 1. Longitudinal torsional compound ultrasonic vibration micro hole drilling system

Longitudinal and torsional compound ultrasonic vibration drilling of tiny deep holes is to apply high frequency longitudinal vibration and torsional vibration to the tool or workpiece during the drilling

ISSN: 2414-1895 DOI: 10.6919/ICJE.202208_8(8).0052

process of tiny deep holes[15,16]. As shown in Figure 1, the ultrasonic generator generates a certain high-frequency sinusoidal electrical signal, and transmits the high-frequency signal generated by the excitation coil fixed on the spindle frame to the induction coil mounted on the rotating shaft through a wireless transmission device, which is connected to the transducer, and converts the received high-frequency electrical signal into the vibration energy of the variable amplitude rod by using the inverse piezoelectric effect of the piezoelectric ceramic in the transducer. The spiral groove on the variable amplitude rod amplifies the amplitude transmitted by the transducer on the one hand, and produces ultrasonic torsional vibration on the other. The ultrasonic vibration in the longitudinal direction and the ultrasonic vibration in the torsional direction are combined to produce elliptical vibration at the tool end[17-20].The section headings are in boldface capital and lowercase letters. Second level headings are typed as part of the succeeding paragraph (like the subsection heading of this paragraph). All manuscripts must be in English, also the table and figure texts, otherwise we cannot publish your paper. Please keep a second copy of your manuscript in your office. When receiving the paper, we assume that the corresponding authors grant us the copyright to use the paper for the book or journal in question. When receiving the paper, we assume that the corresponding authors grant us the copyright to use the paper for the book or journal in question. When receiving the paper, we assume that the corresponding authors grant us the copyright to use.

As shown in Figure 2, the coordinate system is established with the center of the drill bit as the origin. The motion trajectory of any point on the cutting edge of ordinary drilling is obtained as:

$$\left.\begin{aligned} x &= r\bullet\sin\left(2\pi nt\right) \\ y &= r\bullet\cos\left(2\pi nt\right) \\ z &= -f_r t/60 \end{aligned}\right\} \tag{1}$$

Ultrasonic-assisted drilling imposes high-frequency vibration on the drill bit compared with conventional drilling processing. Based on the ultrasonic vibration characteristics, the equation of motion of any point on the cutting edge of longitudinal-torsional composite ultrasonic vibration drilling is established as follows.

$$\left.\begin{aligned} x &= r\bullet\sin\left(2\pi nt+\left(A_2\sin\left(2\pi ft+\varphi\right)\right)/r\right) \\ y &= r\bullet\cos\left(2\pi nt+\left(A_2\sin\left(2\pi ft+\varphi\right)\right)/r\right) \\ z &= -f_r t/60-\frac{A\sin\left(2\pi ft\right)}{1000} \end{aligned}\right\} \tag{2}$$

where x is the displacement of a point on the main cutting edge of the drill along the x axis direction(mm); y is the displacement of a point on the main cutting edge of the drill along the y-axis direction(mm). z is the displacement of a point on the main cutting edge of the drill along z axis direction (mm); r is the distance from any point on the cutting edge of the drill to the axis (mm). fr is the axial feed speed of the drill(mm/min); n is the spindle speed(r/min); f is the vibration frequency of the drill bit(Hz). $\varphi$is the initial phase.A is the longitudinal amplitude; and A2 is the tangential amplitude.

ISSN: 2414-1895 DOI: 10.6919/ICJE.202208_8(8).0052

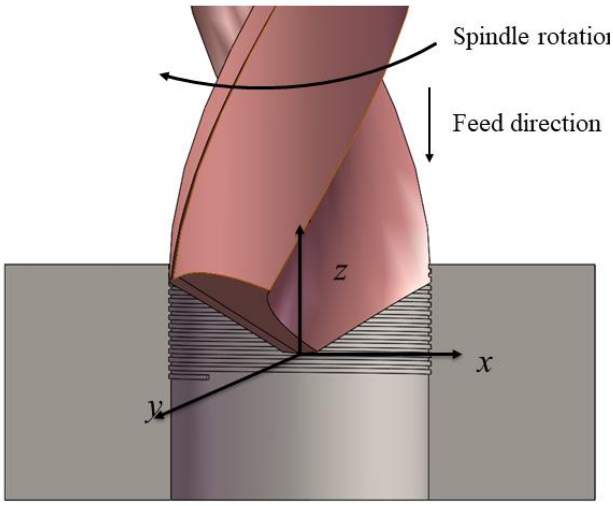

(a) Common micro hole drilling

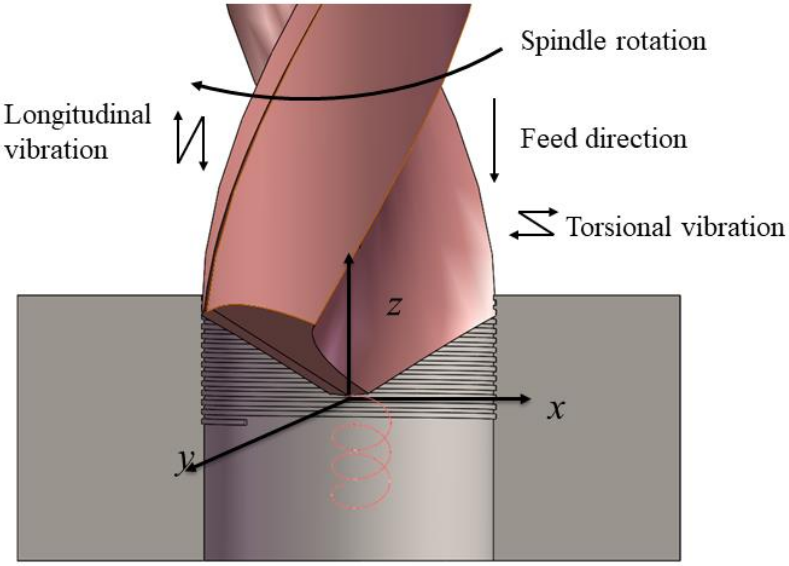

(b) Longitudinal torsional combined ultrasonic vibration drilling

Figure 2. Micro hole drilling model

2.2 Motion Trajectory of the Main Cutting Edge

The analysis of the cutting edge trajectory is one of the important bases for the study of ultrasonic vibration drilling. As shown in Figure 3(a), the trajectory of a point on the main cutting edge during ordinary drilling is a spiral, while longitudinal ultrasonic vibration drilling is a spiral rising sine curve. From the drilling principle, it is clear that the drilling feed rate is much smaller than the tangential speed, and its influence on the instantaneous cutting speed and effective tool geometry angle is smaller, when the feed per revolution is the main influencing factor of axial force and torque. As shown in Figure 3(b), the longitudinal-torsional composite auxiliary drilling is superimposed with high-frequency harmonic vibration in the axial and tangential directions, which adds a change of torsional angle compared with longitudinal drilling, and the direction and size of its cutting speed will change rapidly with the high-frequency harmonic vibration, and the longitudinal-torsional composite ultrasonic vibration changes the instantaneous feed rate, thus causing the instantaneous cutting speed and effective tool geometry angle to change with it, which will have a significant effect on the drilling axial force.

ISSN: 2414-1895 DOI: 10.6919/ICJE.202208_8(8).0052

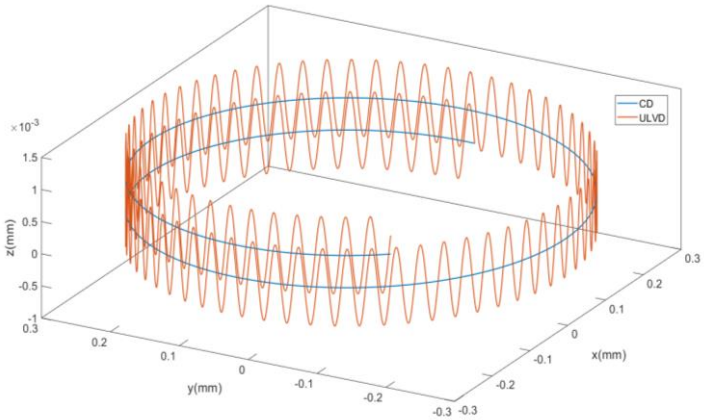

(a) Comparison between conventional drilling and longitudinal ultrasonic vibration drilling

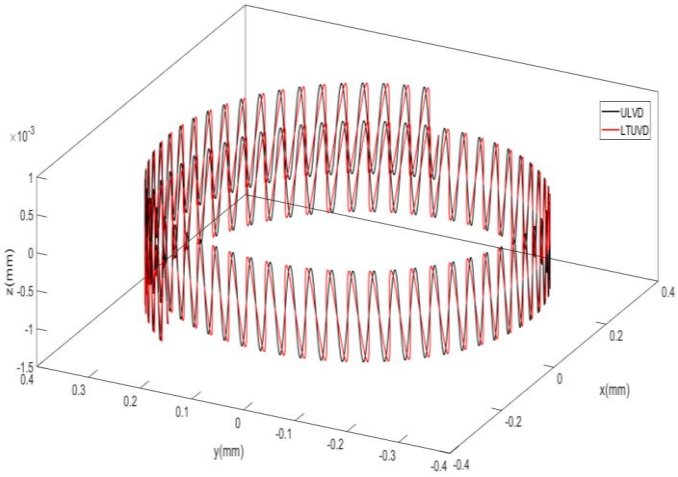

(b) Comparison between longitudinal ultrasonic vibration and longitudinal torsional combined ultrasonic vibration drilling trajectory

Figure 3. Movement track of main cutting edge of drill bit

3. Longitudinal Torsion Compound Ultrasonic Vibration Micro Deep Hole Drilling Dynamics Analysis

3.1 Axial Force Analysis of the Main Cutting Edge of Longitudinal Ultrasonic Vibration Drilling

In micro-hole machining, due to the symmetry of the main cutting edge of the drill, it is generally assumed that the radial forces generated during drilling cancel each other out and the cutting forces are mainly axial. The cutting force is related to the cutting thickness, and since the main cutting edge plays the main removal role when drilling, it is necessary to find out the cutting thickness of the main edge.

As shown in Figure 4, in the longitudinal ultrasonic vibration drilling method, the drill bit performs a constant velocity feed motion in addition to the superimposed axial simple harmonic motion. As shown in Figure 5, in order to analyze the mechanism of axial force generated by the main cutting edge, let the length from the point on the main cutting edge at a distance r from the axis to the inflection point of the transverse edge be l , then:

$$l = \frac{\sqrt{r^2 - (\frac{L_1}{2})^2} - \frac{r_0}{2} sin\psi}{sin\frac{p}{2}} \tag{3}$$

ISSN: 2414-1895 DOI: 10.6919/ICJE.202208_8(8).0052

whereL_1 is the thickness of the drill core (mm); p is the drill sharpness angle (°). r_0 is the cross-edge length (mm).ψ is the cross-edge turning angle (°).

The complex geometry and high-speed motion of the drill bit make it very difficult to accurately represent its overall working state during drilling. Therefore, the micro-element method is used to quantify the cutting force of the cutting edge part of the drill during the drilling process. The micro-element dl with the distance r from the main cutting edge to the axis is taken as the object of study, and the micro-element's Z displacement in the direction of:

$$z(t) = \frac{-Asinft}{1000} - \frac{f_r t}{60} \tag{4}$$

The derivative of the displacement with respect to time t gives the axial vibration velocity:

$$\dot{z}(t) = \frac{-Asinft}{1000} - \frac{f_r t}{60} \tag{5}$$

The main motion of drilling is rotation, and if the change of angle is ignored, the tangential motion can be considered as uniform linear motion if only the magnitude of the tangential motion is analyzed, and noteV_c' is the tangential velocity of the micro element at dl, then:

$$V_c'(r) = \frac{2\pi rn}{60} \tag{6}$$

Let its tangential distance be$x(t)$, then:

$$x(t) = V_c' t \tag{7}$$

Since the tool is rotating at a constant speed, the angle of rotation of the drill is given as θ , then:

$$\theta = \frac{2\pi nt}{60} \tag{8}$$

$$z(\theta) = \frac{-Asin(\frac{60f\theta}{2\pi n})}{1000} - \frac{f_r \theta}{2\pi n} \tag{9}$$

Because there is an axial reciprocating effect of ultrasonic axial vibration, which means that the tool will lift up and no longer cut the material in a certain time, it also indicates that the chip thickness of ultrasonic drilling vibration drilling is not uniform. As shown in Figure 6(a), CD1 and CD2 indicate the cutting trajectory of the previous ordinary drilling and the cutting trajectory of the current ordinary drilling respectively; ULVD1 and ULVD2 indicate the cutting trajectory of the previous vibration drilling and the cutting trajectory of the current vibration drilling respectively. Expanding Fig. 6(a) along the helix as shown in Fig. 6(b), the vertical coordinates indicate the axial displacement, then the straight lines CD1 and CD2 indicate the axial displacement at a point on the main edge during conventional drilling, and the wavy lines ULVD1 and ULVD2 indicate the displacement under vibration drilling, where ULVD1 indicates the trajectory of the previous revolution and ULVD2 indicates the trajectory of the immediately following revolution. Since drilling is done with constant feed, the chip thickness can be expressed as the distance between two adjacent tool trajectories. For conventional drilling, the chip thickness is the distance between two black parallel lines, which can

ISSN: 2414-1895 DOI: 10.6919/ICJE.202208_8(8).0052

be seen to be constant under the conventional drilling method. For ultrasonic axial vibration drilling, the instantaneous chip thickness is the area between the red wavy line and the blue wavy line, and since the drilling feed direction Z is negative, the chip thickness is equal to the spacing between the red wavy line above and the blue wavy line below at any moment, and when the blue wavy line is above the red wavy line, it indicates an empty cutting state with the tool tip raised.

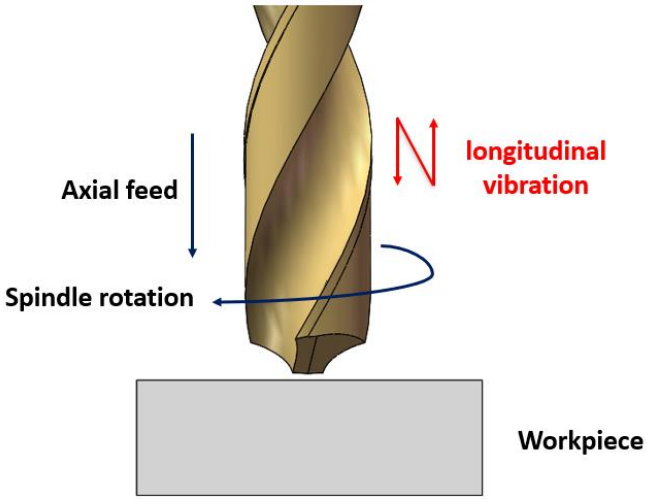

Figure 4. Longitudinal ultrasonic vibration drilling model

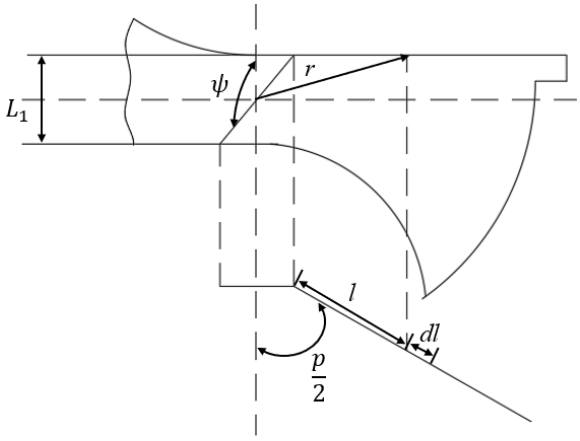

Figure 5. Micro element structure of main cutting edge

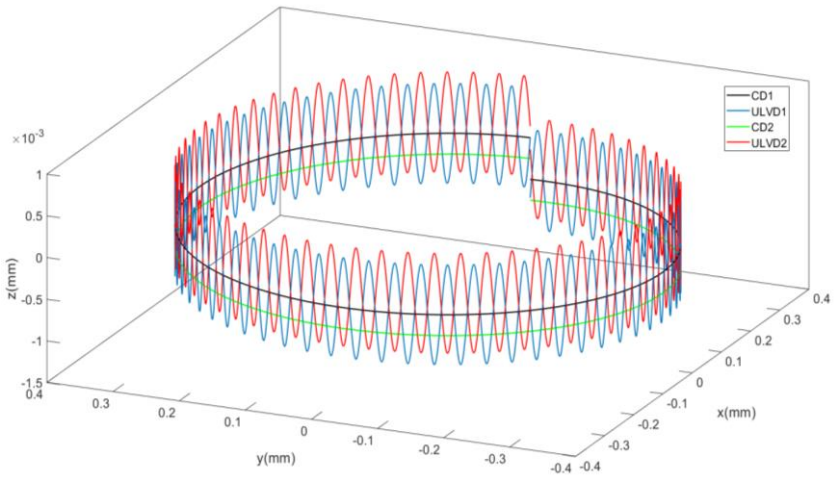

a

Volume 8 Issue 8, 2022
DOI: 10.6919/ICJE.202208_8(8).0052

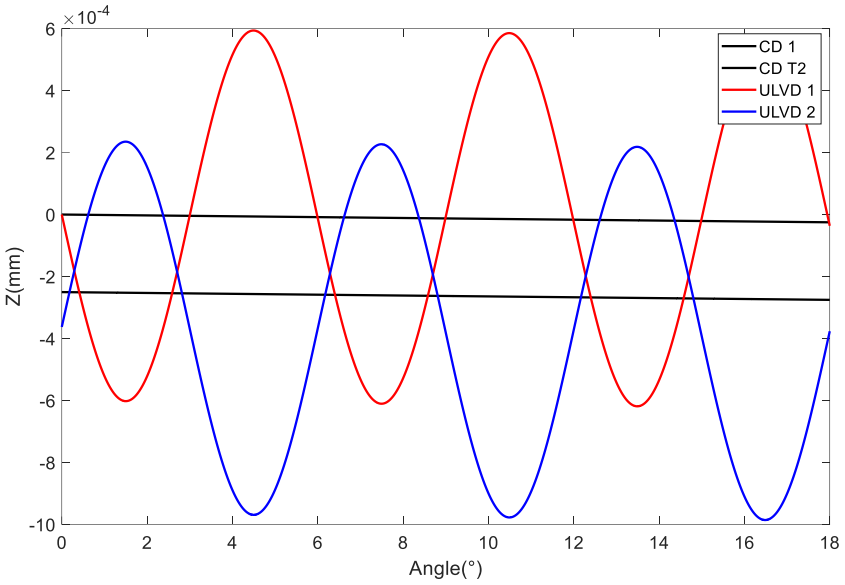

b

Figure 6. Motion trace of two main cutting edges

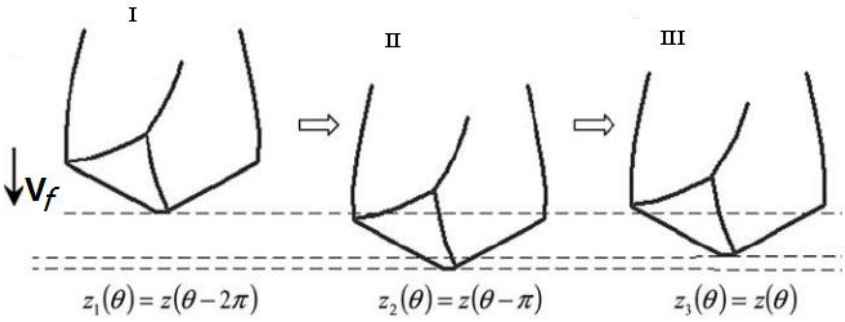

Figure 7. Variation of cutting depth in micro hole drilling

For a double-edged twist drill, the two edges differ by 180° , as shown in Figure 7, when the angular displacement is θ when the axial displacement of the drill bit is $z(\theta)$, due to the presence of ultrasonic vibration, not every time the cutting edge turns to θ cutting will occur when the cutting edge is turned. So when the turning angle is θ When, if we set the axial displacement of the previous time when the cutting edge cut into the material as $z(\theta - m\pi)$, where m is a positive integer, and because the feed direction was previously assumed to be Z the negative direction of the axis, so set θ The "deepest" axial displacement corresponding to the angle is $z_{min}(\theta)$ then:

$$z_{min}(\theta) = z(\theta - m\pi) \tag{10}$$

where m is the minimum positive integer that satisfies $z(\theta - m\pi) < z[\theta - (m+1)\pi]$ the smallest positive integer.

When the drill bit rotation angle is θ The dynamic axial chip thickness when the h_f is.

$$h_f = \begin{cases} z_{min}(\theta) - z(\theta) & \text{When } z(\theta) < z_{min}(\theta) \\ 0 & \text{When } (\theta) \geq z_{min}(\theta) \end{cases} \tag{11}$$

ISSN: 2414-1895 DOI: 10.6919/ICJE.202208_8(8).0052

After finding the cutting thickness, using the binary orthogonal cutting principle, we can find the micro elementdl force applied dF_s : The:

$$h_l = \frac{h_f}{cos\eta_d} sin(k_{rd}) \tag{12}$$

$$dF_s = \frac{K_{AB} h_l dl}{sin\emptyset_{nd}} \tag{13}$$

$$tan\ \eta_d = \frac{\dot{z}}{\dot{x}} = \frac{\frac{-Afcosft}{1000} - V_f}{2\pi nrcos(2\pi nt)} \tag{14}$$

whereh_l is the micro-elementdl the dynamic cutting thickness straight in the working cutting plane.k_{rd} is the dynamic main deflection angle.η_d is the dynamic feed angle.K_{AB} is the shear flow stress, which is a constant determined by the material being cut. $\emptyset_{nd}$ is the micro-elementdl the dynamic shear angle.

3.2 Axial Force Analysis of Longitudinal Torsion Compound Ultrasonic Vibration Drilling

As shown in Figure 3(b), the longitudinal-torsional composite ultrasonic vibration differs from longitudinal ultrasonic vibration drilling in that it exhibits an additional torsional vibration in the tangential direction of the drill bit. For the micro element on the cutting edge dl , its tangential displacement and tangential velocity are as follows:

$$x(t) = \frac{B(r)}{1000} sin(ft) + V_c' t \tag{15}$$

$$\dot{x(t)} = \frac{fB(r)cos(ft)}{1000} + V_c' \tag{16}$$

where$B(r)$ is the dl the tangential amplitude of, $B(r) = Br/R$ is the tangential amplitude of$B$ is the tangential amplitude of the drill bit diameter d is the tangential amplitude at.

With the application of torsional vibration, the tip of the tool has an additional form of motion that extends forward and backward in one vibration cycle, and the dynamic feed angle of the blade compared to the longitudinal vibration η_d has an additional trigonometric component in the denominator of:

$$tan\ \eta_d = \frac{\dot{z}}{\dot{x}} = \frac{\frac{-Afcosft}{1000} - V_f}{\frac{fB(r)sin(ft)}{1000} + V_c'} \tag{17}$$

Micro elements at radius r under longitudinal torsional complex vibration dl at radius r γ_{nd} , dynamic feed front angle γ_{fd} , dynamic main deflection angle k_{rd} and normal front angle γ_n are solved as follows:

$$sin(\lambda_{sd}) = cospsin\eta_d + sin\frac{p}{2} cos\eta_d \tag{18}$$

$$\gamma_{fd} = \gamma_f + \eta_d \tag{19}$$

ISSN: 2414-1895 DOI: 10.6919/ICJE.202208_8(8).0052

$$tan\lambda_{nd} = \frac{tan\lambda_{fd}cos\lambda_{sd}}{sink_{rd}} + \frac{sin\lambda_{sd}}{tank_{rd}} \tag{20}$$

$$tank_{rd} = \frac{sink_r}{cosk_r + tan\lambda_s sin\eta_d} \tag{21}$$

$$\gamma_n = \gamma_f - \xi \tag{22}$$

$$\xi = arctan(tanacosp) \tag{23}$$

$$\gamma_f = arctan\left(\frac{tan\beta cosa}{sinp - cosptan\delta sina}\right) \tag{24}$$

$$\beta = \frac{2r}{D} tan\beta_0 \tag{25}$$

$$a = arcsin\frac{w}{2r} \tag{26}$$

Considering the cutting micro-edge as a small turning tool, the dynamic shear angle can be found from thisϕ_{nd} , the dynamic friction angle λ_{nd} , and dynamic chip flow angle η_{cd} : The:

$$tan\phi_{nd} = \frac{r_l cos\,\eta_{cd} cos\lambda_{nd}}{cos\,\eta_{sd} - r_l cos\,\eta_{cd} sin\lambda_{nd}} \tag{27}$$

$$tan(\phi_{nd} + \lambda_{nd}) = \frac{tan\lambda_{sd} cos\lambda_{nd}}{tan\eta_{cd} - sin\lambda_{nd} tan\lambda_{sd}} \tag{28}$$

$$tan\eta_{cd} = \frac{tan\lambda_{sd} cos\lambda_{nd}}{tan(\phi_{nd} + \lambda_{nd})} + tan\lambda_{sd} sin\lambda_{nd} \tag{29}$$

where r_l is the chip deformation ratio.

Using equation (5), we can finddl and substituting into equation (15), thedF_s is transformed intodr the function of:

$$dF_s = \frac{K_{AB} h_l r}{(sin\phi_n)(sinp)(r^2 - \omega^2)^{\frac{1}{2}}} dr \tag{30}$$

Taking the main edge micro-element dl as the object of study, as shown in Figure 8, it can be seen that the cutting force on the main edge micro-element can be decomposed into$dF_C^{'}$,$dF_T^{'}$ and $dF_R^{'}$ where$dF_C^{'}$ is orthogonal to the main edge and lies in the plane formed by the main edge and V_C in the plane formed by$dF_T^{'}$ is perpendicular to the machined surface, and from the figure it can be seen that $dF_C^{'}$, $dF_T^{'}$ and $dF_R^{'}$ and dF_C , dF_T , and dF_R The relationship between satisfies the following conditions.

Volume 8 Issue 8, 2022
DOI: 10.6919/ICJE.202208_8(8).0052

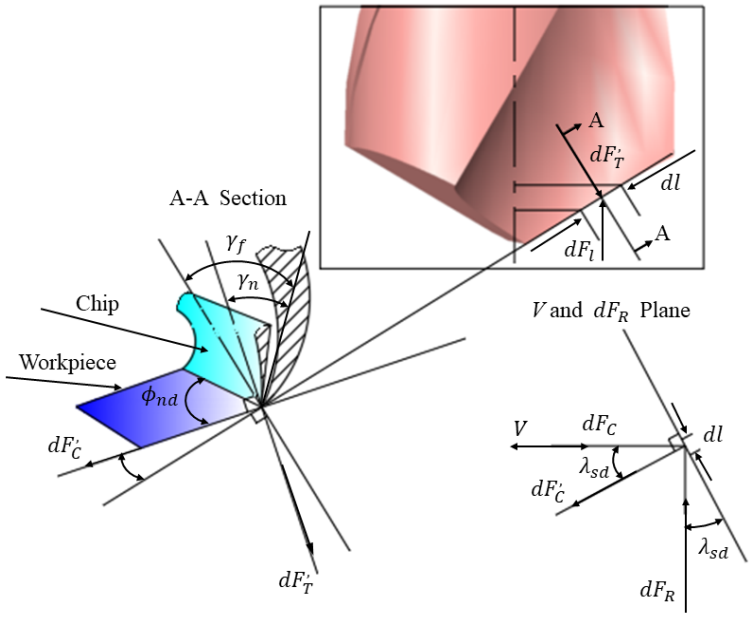

Figure 8. Schematic diagram of each cutting force component on the main cutting edge

$$\left.\begin{aligned} dF_C &= dF_C' \cos\lambda_{sd} + dF_T' \sin\lambda_{sd} \\ dF_T &= dF_T' \\ dF_R &= dF_R' \cos\lambda_{sd} - dF_C' \sin\lambda_{sd} \end{aligned}\right\} \tag{31}$$

It is possible to find the axial force on the main cutting edge dr The axial force on the micro element atdF_l : The:

$$dF_l = [dF_T^2 + (dF_C\cos\lambda_{sd} - dF_R\sin\lambda_{sd})^2]^{\frac{1}{2}}\sin(\lambda_{nd} - \gamma_{nd} - \xi)\sin\frac{p}{2} - (dF_C\sin\lambda_{sd} - dF_R\cos\lambda_{sd})\cos\frac{p}{2} \tag{32}$$

Then the axial force per unit length on the main edge is$\frac{dF_l}{dr}$ and for$\frac{dF_l}{dr}$ The axial force on the entire main cutting edge from the radius of the cross cutting edger_0 to the outer diameter R, the axial force on the main cutting edge is obtained:

$$F_l = \int_{r_0}^{\frac{dD}{2}} \frac{dF_l}{dr} dr \tag{33}$$

For the forces generated by the cross-edge, this is shown in Figure 9. Similar to the model of the main cutting edge, the dynamic normal front angle of the cross-edge is r_{nd}' : The:

$$r_{nd}' = \eta_d' - \gamma_w \tag{34}$$

$$\tan\gamma_w = \tan p \sin\psi \tag{35}$$

ISSN: 2414-1895 DOI: 10.6919/ICJE.202208_8(8).0052

Using the quadratic model, we get:

$$dF_s = \frac{K_{AB}h_c}{sin\phi'_{nd}}dr \tag{36}$$

then the unit cutting force at the distance from the origin of the axis r The unit cutting force of the upper cross-edge micro-element at the origin of the axis isdF_C/dr The cross-edge micro-element is integrated over the interval from 0 to r_0 and the axial force of the cross-edge is obtained as:

$$F_c = \int_0^{r_0} \frac{dF_C}{dr} dr \tag{37}$$

Considering the symmetry, the force of the transverse edge and the force of the main edge are superimposed to obtain the total axial force F.

$$F = 2F_C + 2F_L \tag{38}$$

Using the above equation, the average axial force can be found over a period T F_{mean} : The:

$$F_{mean} = \frac{1}{T}\int_0^T Fdt \tag{39}$$

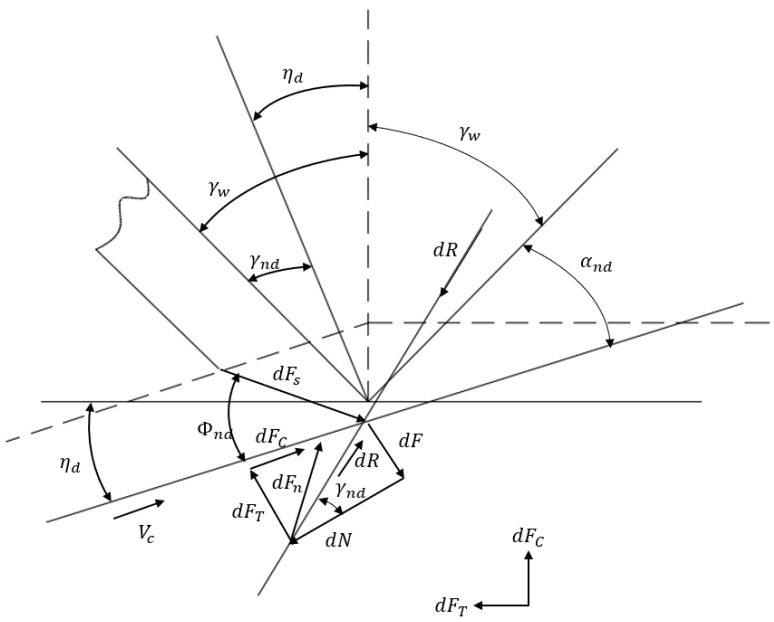

Figure 9. Diagram of force and angle on the cross edge

4. Test Conditions and Equipment

The material used for the experiments is TC4 titanium alloy sheet, the sheet size is 57mm× 15mm× The material parameters are shown in Table 1, and a 0.3mm diameter microfine tungsten alloy drill bit is used in the experiment, with the specific parameters shown in Table 2.

To investigate the effect of machining parameters on ultrasound-assisted micro-hole drilling, a single-factor test was designed as in Table 3.

ISSN: 2414-1895 DOI: 10.6919/ICJE.202208_8(8).0052

A Keyence LK-G10 laser displacement sensor was used to measure the amplitude of the tool end before the test. The Kistler 9257B three-way dynamic voltage force measurement system was used during the test to measure the axial force during the drilling process. After the test, the entrance and exit of the microhole and chips were observed using a Keience VHX-2000 digital microscope, and the hole wall was observed using a Merlin Compact scanning electron microscope.

Table 1. Test site diagram TC4 titanium alloy performance parameters

Density (Kg/m^3)	Conductivity (w/m*k)	Young's modulus E/(GPa)	Poisson's ratio	Specific heat capacity J/(kg*° C)	Expansion coefficient	Inelastic heat fraction
4400	6.8	112	0.34	611	9.32E-6	0.9

Table 2. Tool parameters

Diameter D(mm)	Cross blade length L_1(mm)	Cross-edge corner ψ(°)	Drill core thickness s(mm)	Cross blade length D_1 (mm)	Crest angle p(°)	Spiral Angle β_0(°)
0.35	0.16	140	0.10	0.06	120	50

Table 3. Machining parameters

Spindle peed (r/min)	Feed rate (μm/r)	A (μm)	A_2 (μm)
12000/16000/20000/24000	5/10/15/20	0/0.6/0.8/1/1.2	0.8

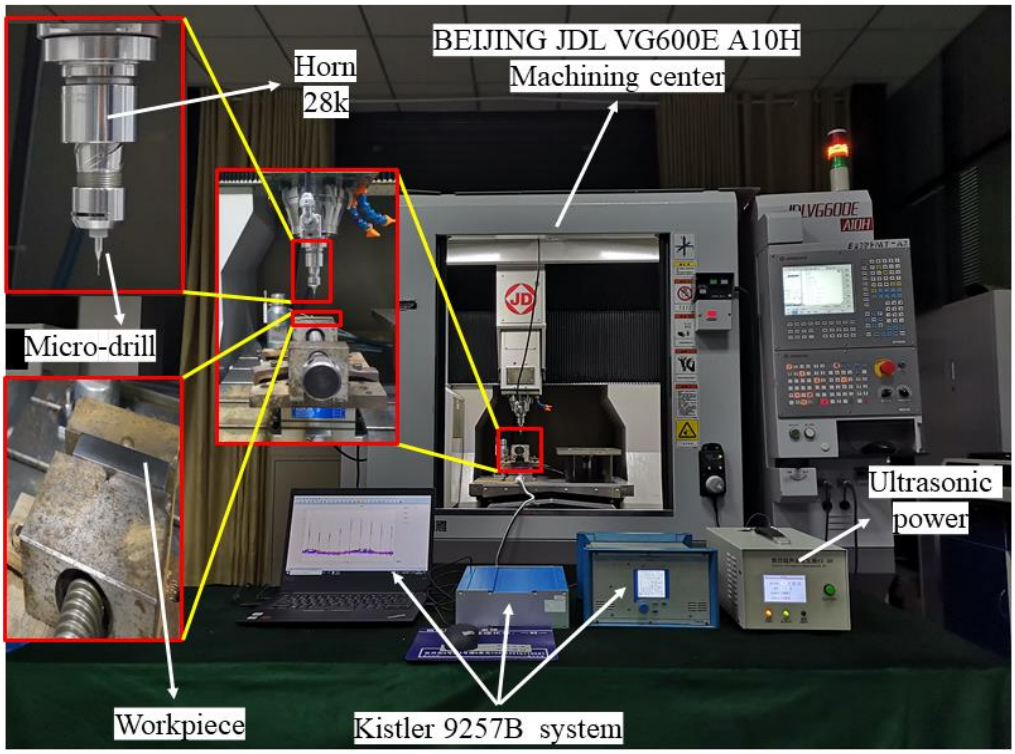

Fig.10 Schematic siagram of Experiment site

ISSN: 2414-1895 DOI: 10.6919/ICJE.202208_8(8).0052

5. Experimental Results and Analysis

The drilling process is divided into three stages: drilling in, drilling in and drilling out, and the drilling force was measured by using the Kistler 9257B three-way dynamic voltage type force measurement system. Figure 11(a) shows the general drilling axial force waveform, and Figure 11(b) shows the longitudinal-torsional composite ultrasonic vibration drilling axial force waveform.

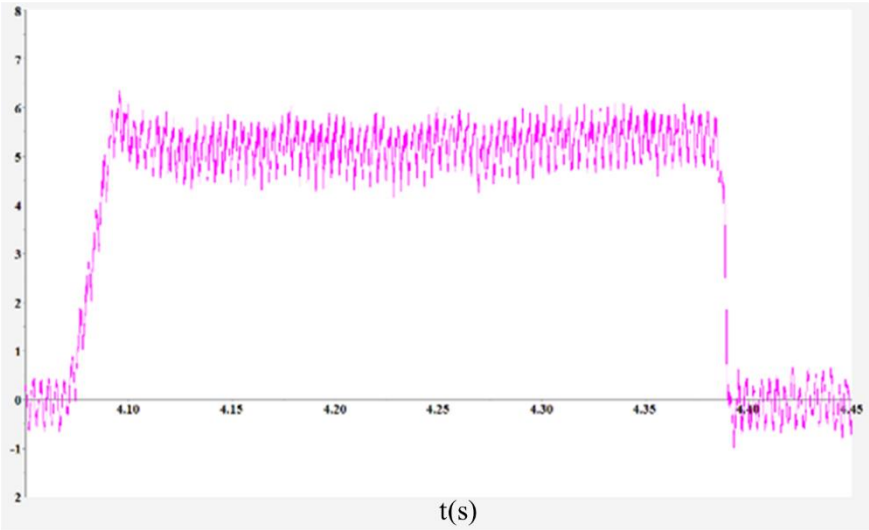

a Common drilling

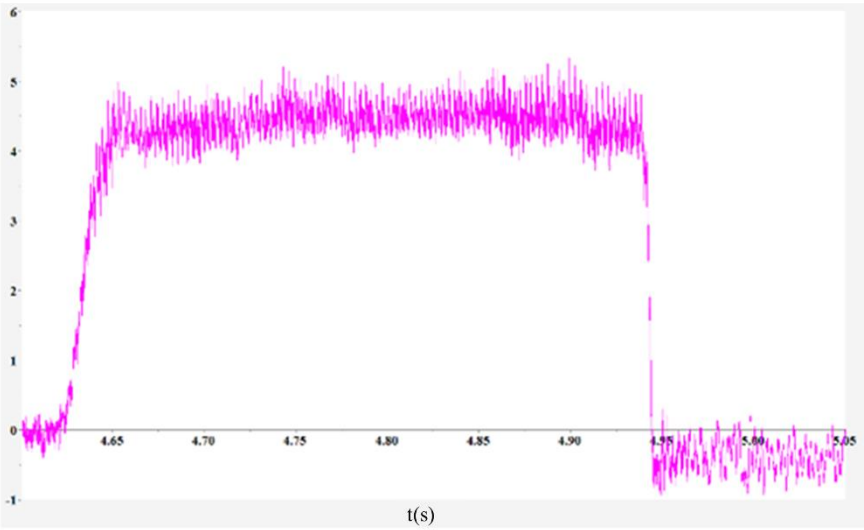

b Longitudinal torsional combined ultrasonic vibration drilling

Figure 11. Waveform of drilling axial force

The test was conducted by beak drilling, and five sets of axial force data were averaged for each hole during steady drilling. As shown in Figure 12, the axial force tends to decrease with the increase of spindle speed regardless of the machining method; when the speed exceeds 20,000 r/min, the trend of LTUAD axial force decreasing with the increase of speed slows down; the axial force of LTUVD decreases 15.7%~26.5% than that of CD.

This is mainly due to the increased chip breaking and outflow capability, chip breaking and miniaturization alleviating tool wear as the cutting edge moves along an elliptical trajectory during LTUVD TC4 titanium alloy. As shown in Fig. 3(b), after the torsional vibration is applied, there exists axial and tangential reciprocating motion of the cutting edge, and the cutting edge has an

Volume 8 Issue 8, 2022
DOI: 10.6919/ICJE.202208_8(8).0052

additional form of forward extension and backward motion attached to one vibration cycle, compared with ordinary drilling, the dynamic feed angle of the cutting edge η_d becomes larger, which is the main reason for the decrease of axial force. On the other hand, compared with ordinary drilling, the torsional vibration of the tool tip makes the maximum speed of the cutting edge per unit cycle greater, which in turn has a stronger impact effect and is more conducive to breaking the chips, reducing tool wear and lowering the axial force.

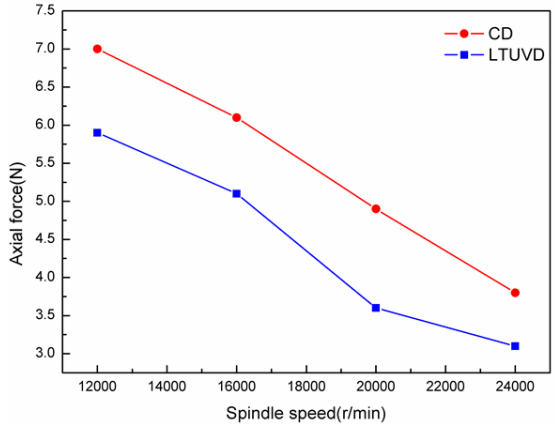

Figure 12. Influence of spindle speed on axial force

The effect of feed rate on the axial force is shown in Figure 13. It can be seen that LTUAD has the lowest axial force at a feed of 0.25 μm/r when the axial force is the smallest, only 2.5N; and the LTUAD axial force is significantly lower compared to CD. As shown in Figure 8, because of the constant feed when drilling, the chip thickness can be expressed by the spacing between two adjacent tool trajectories; for CD, the chip thickness is the distance between two blue parallel lines, and it can be seen that the chip thickness is constant in this drilling method; for LTUAD, there is an axial reciprocating effect of ultrasonic axial vibration, which means that the tool will lift up and no longer cut the material in a certain time. There is the phenomenon of empty cutting, which is the reduction of tool wear and thus the reduction of axial force; and the chip thickness of LTUAD is not uniform.

The effect of feed rate on axial force is mainly reflected in the chip thickness, whether it is CD or LTUAD, with the increase of feed rate, the chip thickness increases, which leads to the increase of axial force.

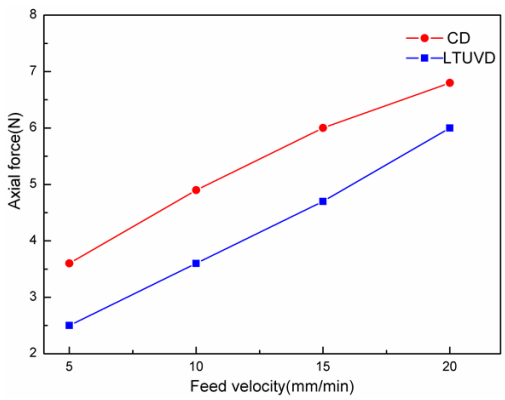

Figure 13 Effect of feed speed on axial force

From Figure 14, it can be seen that the effect of LTUAD amplitude on axial force is weakening, and it is important to select the appropriate amplitude value to improve the machining quality and machining efficiency of micro-hole.

Volume 8 Issue 8, 2022
DOI: 10.6919/ICJE.202208_8(8).0052

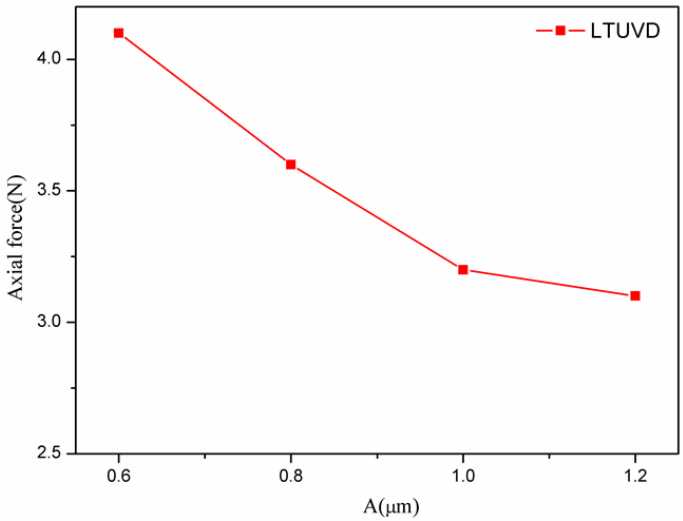

Figure 14. Effect of ultrasonic amplitude on axial force

5.1 Chip Analysis

The cuts during the experiments were collected and observed with an ultra-spiritual microscope. As shown in Figure 15, it can be clearly seen that under the same cutting parameters, after the application of longitudinal vibration, due to the discontinuous cutting mode of "contact-separation-contact" between the tool and the workpiece in ultrasonic vibration-assisted drilling, the cutting is more likely to break, and the machining produces smaller cutting and easier to exclude; under ordinary drilling, the chips It is not easy to fracture, and even the phenomenon of chip winding is generated. Under high speed rotation, the entangled chips will scratch the hole wall, not easy to separate from the drill bit, and will rotate and entangle at the entrance of the micro-hole, seriously damaging the entrance shape.

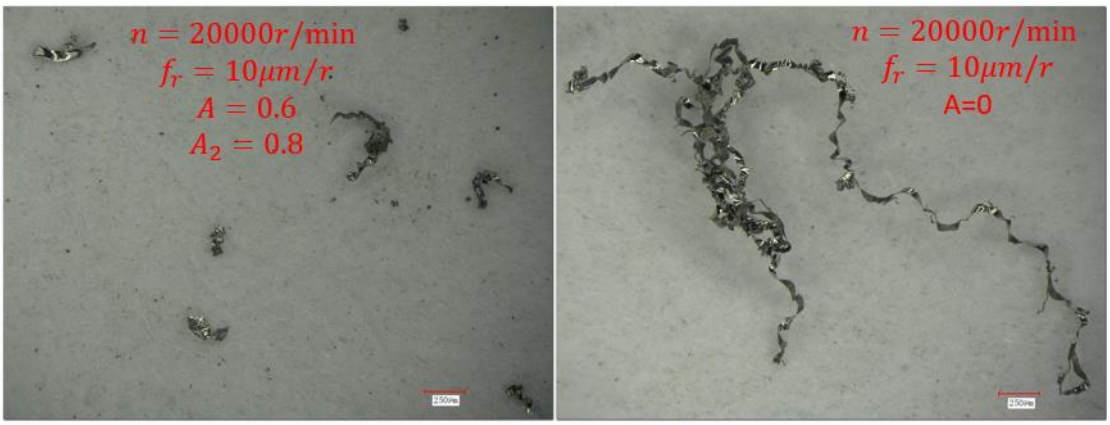

Figure 15. Chip shape

6. Conclusion

1) A longitudinal-torsional composite ultrasonic vibration drilling model was established based on the cyclic characteristics of ultrasonic waves and the drilling principle. The effect of ultrasonic-assisted drilling on the cutting thickness was analyzed. The axial force model of the main cutting edge and cross edge under longitudinal torsional composite ultrasonic vibration drilling was solved by using the micro-element method. And the rationality of the axial force model under the longitudinal-torsional composite ultrasonic vibration conditions was analyzed by micro-hole drilling tests.

ISSN: 2414-1895 DOI: 10.6919/ICJE.202208_8(8).0052

2) Longitudinal torsional composite ultrasonic vibration micro-hole drilling can significantly reduce the magnitude of axial cutting forces compared to ordinary drilling of micro-hole. The improvement effect of longitudinal torsion compound ultrasonic vibration drilling micro-hole on axial force does not increase with the increase of amplitude; on the contrary, too large amplitude may not increase the improvement effect.

3) When ultrasonic longitudinal torsion compound vibration drilling micro-hole, the burr is smaller and easier to fracture.

References

[1] Materials Research; Researchers' Work from Jiangnan University Focuses on Materials Research (Effect of Laser Rescanning on the Characteristics and Residual Stress of Selective Laser Melted Titanium Ti6Al4V Alloy)[J]. Chemicals & Chemistry,2020.

[2] Jitupan Sarma,Ramanuj Kumar,Ashok Kumar Sahoo,et al. Enhancement of material properties of titanium alloys through heat treatment process: A brief review[J]. Materials Today: Proceedings,2020,23(Pt 3).

[3] Gao Tiejun,Wang Kaifeng,Ling Zhiyuan,et al. Effect of a Compound Energy Field with Temperature and Ultrasonic Vibration on the Material Properties and Bending Process of TC2 Titanium Alloy[J]. Materials,2021,14(23).

[4] James C. Williams,Rodney R. Boyer. Opportunities and Issues in the Application of Titanium Alloys for Aerospace Components[J]. Metals,2020,10(6).

[5] N. A. Nochovnaya,P. V. Panin,E. B. Alekseev,K. A. Bokov. Modern Sparingly Alloyed Titanium Alloys: Application and Prospects[J]. Metal Science and Heat Treatment,2017,58(9-10).

[6] Editorial: Titanium Alloys: Properties, Processing and Applications[J]. Advanced Engineering Materials, 2017,19(6).

[7] Suman Chatterjee,Siba Sankar Mahapatra,Kumar Abhishek. Simulation and optimization of machining parameters in drilling of titanium alloys[J]. Simulation Modelling Practice and Theory,2016,62.

[8] Takashi Matsumura,Shoichi Tamura. Cutting Simulation of Titanium Alloy Drilling with Energy Analysis and FEM[J]. Procedia CIRP,2015,31.

[9] Zhang Feng Liu,Pei Xuan Yang. Titanium Alloy Ultrasonic Vibration Micro Deep Holes Drilling[J]. Advanced Materials Research,2014,3381(1004-1005).

[10] Zhu Lin,Li Ji Yun. Experimental Research on the Surface Roughness Characteristics in Ultrasonic Vibration Lapped Surface of Titanium Alloy[J]. Applied Mechanics and Materials,2010,43(43-43).

[11] Feng P , Wang J , Zhang J , et al. Drilling induced tearing defects in rotary ultrasonic machining of C/SiC composites[J]. Ceramics International, 2017, 43(1):791-799.

[12] Zhong bo, Zhang yukun,Liu kaiqiang. Research on precision deep hole drilling process of ocr17ni4cu4nb stainless steel [j] Shandong youth, 2015, 000 (011): 129-131.

[13] Zhang J , Zhang M L . Simulation Research of Ultrasonic Vibration Micro Hole Drilling Based on Advant Edge FEM[J]. Machinery Design & Manufacture, 2019.

[14] D Schnabel, E ?Zkaya, D Biermann,. Transient Simulation of Cooling-Lubricant Flow for Deep-Hole Drilling-Processes[J]. Procedia CIRP on SciVerse ScienceDirect, 2018.

[15] Yang W , Xu J , Wu Y. Chemical-Mechanical Polishing Principle and Experimental System of Ultrasonic Elliptic Vibration[J]. Journal of Nanjing University of Aeronautics & Astronautics, 2008, 40(6): 753-757.

[16] Huang D Z . Principle of Vibration of Ultrasonic Wave and its Application in Thermal Power Plant[J]. Power System Engineering, 2003.

[17] Li X H , Wang Z , He X H . Influence Principle of Ultrasonic Vibration on the Rheological Behavior of Materials[J]. Advanced Materials Research, 2012, 538-541:1393-1402.

[18] Moriwaki T , Shamoto E . Ultrasonic Elliptical Vibration Cutting[J]. CIRP Annals - Manufacturing Technology, 1995, 44(1):31-34.

ISSN: 2414-1895 DOI: 10.6919/ICJE.202208_8(8).0052

[19] Suzuki N , Nakamura A , Shamoto E , et al. Ultraprecision Micromachining of Hardened Steel by Applying Ultrasonic Elliptical Vibration Cutting[C]// International Symposium on Micro-nanomechatronics & Human Science. IEEE, 2003.

[20] Ma C , Shamoto E , Moriwaki T . Study on the improvement of machining system stability by applying ultrasonic elliptical vibration cutting[J]. Binggong Xuebao/Acta Armamentarii, 2004, 25(6):752-756.